Distribution and Elimination of the Glycosidase Inhibitors 1-Deoxymannojirimycin and *N*-Methyl-1-Deoxynojirimycin in the Rat *in Vivo*

Esther D. Faber,[1,3] Roelof Oosting,[1] Jacques J. Neefjes,[2] Hidde L. Ploegh,[2] and Dirk K. F. Meijer[1]

Received October 23, 1991; accepted March 18, 1992

We studied the pharmacokinetics of two synthetic derivatives of 1-deoxynojirimycin in the rat after intravenous administration. The mannosidase IA/B inhibitor 1-deoxymannojirimycin and the glucosidase inhibitor *N*-methyl-1-deoxynojirimycin exhibited minimal plasma protein binding and showed a rapid biphasic plasma disappearance, with an initial $t_{1/2}$ of 3.0 and 4.5 min, respectively, and a terminal $t_{1/2}$ of 51 and 32 min, respectively. For both compounds renal excretion is the major route of elimination. After 120 min, 52% of the dose of 1-deoxymannojirimycin and 80% of the dose of *N*-methyl-1-deoxymannojirimycin was recovered unchanged from the urine, whereas only 4.9 and 0.2%, respectively, of the dose was excreted in bile. Urinary clearance of 1-deoxymannojirimycin was similar to the glomerular filtration rate. In contrast, urinary clearance of *N*-methyl-1-deoxynojirimycin was two to three times higher than the glomerular filtration rate, indicating active tubular secretion. Ligation of the renal vessels decreased the total-body clearance of 1-deoxymannojirimycin and *N*-methyl-1-deoxynojirimycin 18- and 24-fold, respectively. Neither alkalinization of the urine by infusion of bicarbonate solutions nor forced diuresis altered the renal excretion rate of these compounds, implying the absence of tubular reabsorption. At 120 min, the amounts of 1-deoxymannojirimycin in liver and kidney were 2.1 and 1.1% of the dose, respectively, while small intestine, stomach, and heart contained only 0.9, 0.6 and 0.1%. Less than 1% of the dose of *N*-methyl-1-deoxynojirimycin was found in the collected organs 2 hr after injection. At the same time point, the kidney/plasma concentration ratio of *N*-methyl-1-deoxynojirimycin was 10-fold higher than in other tissues, whereas for 1-deoxymannojirimycin it was only 2- to 3-fold higher in kidney, indicating a more persistent general tissue retention of 1-deoxymannojirimycin.

KEY WORDS: 1-deoxymannojirimycin; *N*-methyl-1-deoxynojirimycin; glycosidase inhibitors; pharmacokinetics; *in vivo;* intravenous administration.

INTRODUCTION

Glycosidase inhibitors block the biosynthesis of N-linked glycan structures, and hence serve to study the function of protein-bound carbohydrates (1,2), such as the role of oligosaccharide trimming in the synthesis and secretion of glycoproteins (3–5). Glycosidase inhibitors also constitute a class of potential therapeutic agents: They have been used as antihyperglycemic compounds (6,7) and inhibitors of tumor metastasis (8) and currently are tested for their antiviral activity (9,10).

Although rather diverse, the glycosidase inhibitors all resemble potential transition-state intermediates of the hydrolytic reactions (1,11). Among the two major inhibitor classes are the indolizidine polyhydroxyalkaloids castanospermine and swainsonine, which inhibit glucosidase I and mannosidase II, respectively (1,2,12), and the nojirimycin piperidine polyhydroxyalkaloids. Nojirimycin, 1-deoxynojirimycin (dNM), and *N*-methyl-1-deoxynojirimycin (MedNM) are glucosidase inhibitors (1,2), while the 2-epimer, 1-deoxymannojirimycin (dMM), is a mannosidase IA/B inhibitor (1,13). The compounds investigated in the present study, MedNM and dMM, are synthetic derivatives of dNM (Fig. 1).

Glycosylation inhibitors have been thoroughly tested *in vitro* with the use of cell cultures (9–11), freshly isolated cells (14,15), or isolated enzymes (6,16,17), but only a few studies deal with the effects of glycosidase inhibitors *in vivo*, including the inhibition of sucrase by selected glucosidase inhibitors in the rat (6), the toxicity of castanospermines in mice (18), and the effect of the α-glucosidase inhibitor miglitol on blood glucose levels in Type II diabetic patients (7). The pharmacokinetics of these inhibitors remained unexplored, even though the antiviral effect of dNM, castanospermine, and analogues are promising. In the present paper we studied the pharmacokinetics of two glycosidase inhibitors, MedNM and dMM, after intravenous injection in male Wistar rats.

MATERIALS AND METHODS

Materials

Deoxymannojirimycin (dMM; 1,5-dideoxy-1,5-imino-D-mannitol), *N*-methyl-deoxynojirimycin (MedNM; *N*-methyl-1,5-dideoxy-1,5-imino-D-glucitol), and the corresponding radioactive compounds were obtained from the Netherlands Cancer Institute, in cooperation with Organon International, Oss, The Netherlands. 1-[^{3}H]dMM (sp act, 25 Ci/mmol) was synthesized as described (11). [^{14}C]MedNM was prepared from 1-deoxynojirimycin (dNM) by means of a reductive alkylation as follows: 26 μmol dNM in 40 μl formic acid was mixed with 32 μmol (500 μCi) [^{14}C]formaldehyde (sp act, 15.5 mCi/mmol; 50 μl, 1–3%, v/v, in H_2O). The mixture was incubated for 24 hr at 80°C. After further addition of 20 μl formic acid, incubation for 50 hr, and purification by Dowex as described (19), the yield of MedNM was 60%. The specific activity of [^{14}C]MedNM was calculated to be 15 mCi/mmol; by mass spectrometry it was determined to be 14.5 mCi/mmol. The purity of the preparation was 98%, as checked by thin-layer chromatographic (TLC) analysis. The structures of both control MedNM and radioactive MedNM were confirmed with ^{1}H-NMR.

Animal Studies

Male Wistar rats (outbred strain, CDL, Groningen, The

[1] Department of Pharmacology and Therapeutics, University Centre for Pharmacy, University of Groningen, Ant. Deusinglaan 2, 9713 AW Groningen, The Netherlands.
[2] The Netherlands Cancer Institute, Plesmanlaan 121, 1066 CX Amsterdam, The Netherlands.
[3] To whom correspondence should be addressed.

0724-8741/92/1100-1442$06.50/0

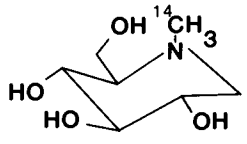

N-Methyldeoxynojirimycin

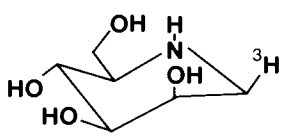

Deoxymannojirimycin

pKa	6.3	7.2
P	0.004	0.016
Protein Binding	0%	5.1%
% Protonized at pH 7.4	9%	39%

Fig. 1. The chemical structures, the position of the radioactive label, and some physicochemical parameters of MedNM and dMM. *P* (partition coefficient octanol/Krebs) and protein binding are determined as described under Materials and Methods. The percentage of the compound that is ionized at any pH can be calculated with the Henderson-Hasselbach equation for bases.

Netherlands) were maintained on rat chow (Hope Farms) and tap water ad libitum in a temperature-controlled chamber at 24°C with a 12-hr light/dark cycle. Rats were fasted overnight, weighing 271 ± 6 g (n = 28) just before the experiment, and anesthetized with pentobarbitone sodium (0.3 ml i.p. of a solution of 60 mg/ml; maintenance dose, 0.05 ml). Animals were prepared for experiments as described by Neef *et al.* (20), with slight modifications. The trachea was intubated to facilitate respiration. The carotid artery was cannulated with a polyethylene canula (ID, 0.5 mm; OD, 1.0 mm) for rapid blood sampling and simultaneous monitoring of blood pressure (HSE electromanometer, March-Hugstetten, FRG). Blood pressure was 80–120 mm Hg in all experiments, except where the renal vessels were ligated (slow decrease to 40 mm Hg). A similar canula was placed in the jugular vein for administration of drug and for infusion of solutions, via an infusion apparatus (Perfusor VI, Braun). Infusions were started 30 min prior to administration of the drug, a period allowed for stabilization. Bile duct and urinary bladder were cannulated as described (21). Bile flow was solely dependent on the endogenous supply of bile salts. Bile and urine samples were collected at 10-min intervals. Body temperature (37.5–38.5°C) was maintained by placing the animal on a heating pad and monitoring its rectal temperature. Four types of experiments were performed.

Mannitol Infusion. Osmotic diuretic mannitol (Merck) was administered as a 5% (isoosmotic) solution in distilled water (1-ml bolus, followed by an infusion of 1.9 ml/hr) to obtain a constant urine flow, as normally urine flow is irregular (22). These experiments were used for baseline investigations and as controls for experiments designed to manipulate urinary clearance. [^{14}C]Mannitol (Amersham), mixed with cold mannitol to a final concentration of 5% (sp act, 28.8 Bq/μmol), was infused to calculate the glomerular filtration rate (GFR) of the kidneys, since the clearance of mannitol approximates the GFR.

Saline Infusion. A solution of 0.154 *M* NaCl (Merck) was infused as an alternative approach to obtain constant urine flow (1-ml bolus, followed by 3.8 ml/hr), to exclude the possibility that mannitol affects the *in vivo* distribution of the structurally similar dMM or MedNM.

Bicarbonate Infusion. Infusions of $NaHCO_3$ (Merck) were administered with mannitol, to raise the pH of urine. A 10% solution of $NaHCO_3$ was infused during the stabilization period (at 3.8 ml/hr), followed by a 1.4% solution (isoosmotic with serum; 1.9 ml/hr) during the experiment. In total, approximately 240 mg of $NaHCO_3$ was administered.

Ligated Renal Vessels. In these experiments, no infusions were given and the renal blood vessels were ligated to exclude renal elimination.

All drugs were given as a bolus dose of 4 μmol in 0.2 ml 0.154 *M* NaCl solution, freshly prepared (35–75 kBq [^{14}C]MedNM, 65–90 kBq [^{3}H]dMM). Blood samples of 0.2 ml were taken 1 min before administration and 2, 4, 6, 10, 20, 30, 60, 90, and 120 min after administration (1 and 45 min were optional). A similar volume of heparinized 0.154 *M* NaCl solution was brought back in the general circulation for fluid replacement. After 2 hr animals were sacrificed and liver, kidneys, small intestine, stomach, and heart were dissected out and treated as described under Radiochemical Tissue Analysis.

Metabolism Studies

TLC was performed on bile and urine samples from additional *in vivo* experiments. Further, the stability of dMM and MedNM was examined in blank bile and urine, before and after incubation for 1 day to 3 weeks. The TLC method was adapted from Neefjes *et al.* (11), with a slight modification of the mobile phase, 2-propanol:H_2O:ammonia (25%) = 80:20:0.5 (v/v/v). The stationary phase consisted of Kieselgel$_{60}$ plates (Merck; 20 × 20 × 0.025 cm). Detection was performed by scanning of radioactivity on a Dünnschichtscanner II LB2723 (Berthold).

Radiochemical Tissue Analysis

[^{14}C]- and [^{3}H]-containing compounds were determined by liquid scintillation counting in plasma, bile, urine, and tissue homogenates as described below. All samples were counted for 5 min in a Beckman LS 1701 liquid scintillation counter. Counting was corrected for quenching by external standardization. Blood samples were collected in heparinized tubes and centrifuged. One hundred microliters of plasma were thoroughly mixed with 4 ml of scintillator (Safe Fluor S, Lumac, Landgraaf, The Netherlands). Bile and urine flow was determined gravimetrically using tared collection vials at 10-min intervals. Each 10-min fraction was mixed with 4 ml of scintillator as above and counted. The liver, kidneys, small intestine, stomach, and heart were dissected out, weighed, and cut into pieces. The tissues were homogenized in a four-fold volume of saline and weighed and an aliquot was mixed with scintillation fluid and counted (in triplicate).

Protein Binding

Binding of the glycosidase inhibitors to plasma proteins was determined in rat plasma, after incubation for 1.5 hr at 37°C, using the Amicon Micropartition I System (Amicon B.V., Rotterdam, The Netherlands), according to the instructions of the manufacturer.

Partition Coefficient

In order to study the lipophilicity of glycosidase inhibitors, the octanol/Krebs partition coefficient was determined as described (23), in an *n*-octanol and Krebs solution system (final concentration of glycosidase inhibitor, 400 μ*M*) from which CO_2 and $NaHCO_3$ were omitted. The pH was adjusted to 7.4 with NaOH.

Pharmacokinetic Analysis

Plasma concentration–time curves were analyzed with the computer program MULTIFIT. This iterative least-squares regression program determines slopes and intercepts of the logarithmically plotted curves of multiexponential functions. The program derives the best-fitting curve and corresponding pharmacokinetic parameters and, also, provides a statistical evaluation (*F* test) of the choice of the model yielding the best fit of the plasma decay curve.

The results of this study were analyzed by simultaneous fitting of all plasma concentration–time curves for each experimental situation. In this way all data pairs are used (instead of a maximum of 11 data pairs for the mean curve) to obtain the most reliable calculation of the kinetic parameters (as shown in Table I; upper section), since the number of "degrees of freedom" for the calculation is highly increased. The program estimates the standard error of the parameters half-life and clearance. For comparison, the mean curve for each experimental situation was fitted also with MULTIFIT.

In the case of linear kinetics, plasma drug concentration at any time t after an intravenous bolus dose is given by

$$C = \sum_{i=1}^{n} C_i \times e^{-\lambda_i \times t} \quad (1)$$

where λ_i is the exponent of the ith exponential term, C is the plasma concentration, and C_i is the initial concentration of the ith component of the curve.

The rate of biliary or urinary excretion (dA_e/dt) is related to the plasma concentration (C) by

$$\frac{dA_e}{dt} = \mathrm{Cl} \times C \quad (2)$$

where the clearance (Cl) is hepatic (Cl_H) or renal (Cl_R), respectively. The hepatic and renal clearance values shown in Table I (middle and lower sections) are calculated this way for each experimental condition from the mean biliary and urinary excretion rates, respectively. The time period from 40 to 80 min was taken (equilibrium conditions), which was divided into four intervals, and the average amount excreted was divided by the average plasma concentration on the midpoint of the sampling interval (mean ± SD of four time intervals).

Total plasma clearance, calculated after simultaneous fitting of all plasma curves, is given by

$$\mathrm{Cl} = \frac{\mathrm{Dose}}{\mathrm{AUC}} \quad (3)$$

The area under the curve (AUC) was calculated from the integral of multiexponential functions [Eq. (1)], from $t = 0$ to $t = \infty$.

Under steady-state conditions total plasma clearance is given by

$$\mathrm{Cl_{ss}} = \frac{R_0}{C_{ss}} \quad (4)$$

in which R_0 is the infusion rate and C_{SS} the plasma concentration at steady-state. This equation is used to calculate the clearance of [^{14}C]mannitol.

Under steady-state conditions the distribution volume V_{SS} (theoretically, the amount of drug in the body divided by the plasma concentration at steady-state) was estimated with

$$V_{ss} = V_1 + V_2 = V_1 \left(1 + \frac{k_{12}}{k_{21}}\right) \quad (5)$$

where V_1 and V_2 are the volumes of distribution of the central and the peripheral compartment, respectively, and k_{12} and k_{21} are the intercompartmental rate constants. This distribution volume parameter is independent of the elimination processes. The V_β (volume of distribution of the elimination phase) was calculated by the fitting program as

$$V_\beta = \frac{\mathrm{Cl}}{\lambda_z} \quad (6)$$

where λ_Z is the smallest value of λ_i in Eq. (1).

The analysis described above is valid only under first-order kinetic conditions (20). For both compounds the concentration independency was checked in the dose range from 4 to 20 μmol. Plasma disappearance and excretion rate patterns for both compounds in this dose range indicated the absence of saturation phenomena.

Statistical Analysis

Statistical evaluation was performed with the unpaired, two-sided Student's *t* test, using the FarmStat 1.10 computer program developed in our laboratory. $P < 0.05$ was the minimal level of statistical significance. Data are given as mean ± SE, unless stated otherwise.

RESULTS

The octanol/Krebs partition coefficient indicates that both dMM and MedNM are hydrophilic, whereas dMM is four times more lipophilic than MedNM (Fig. 1). Plasma protein binding over a concentration range of 40–400 μ*M* was small (5.1%) for dMM and negligible for MedNM.

1-Deoxymannojirimycin

After intravenous administration of [^{3}H]dMM, radioactivity was eliminated from the plasma in a biexponential fashion (Figs. 2A and 3A), with an initial half-life ($t_{1/2_1}$) of 3.0 ± 1.7 min and a terminal half-life ($t_{1/2_2}$) of 51 ± 12 min under control conditions (mean ± SD of six experiments; from simultaneous fitting as described under Materials and Methods). Figure 2A shows that the compound appeared in urine almost instantaneously and in high amounts. The decrease in urinary excretion rate closely followed the decrease in plasma concentration. After 30 min, an average of 28 ± 8%

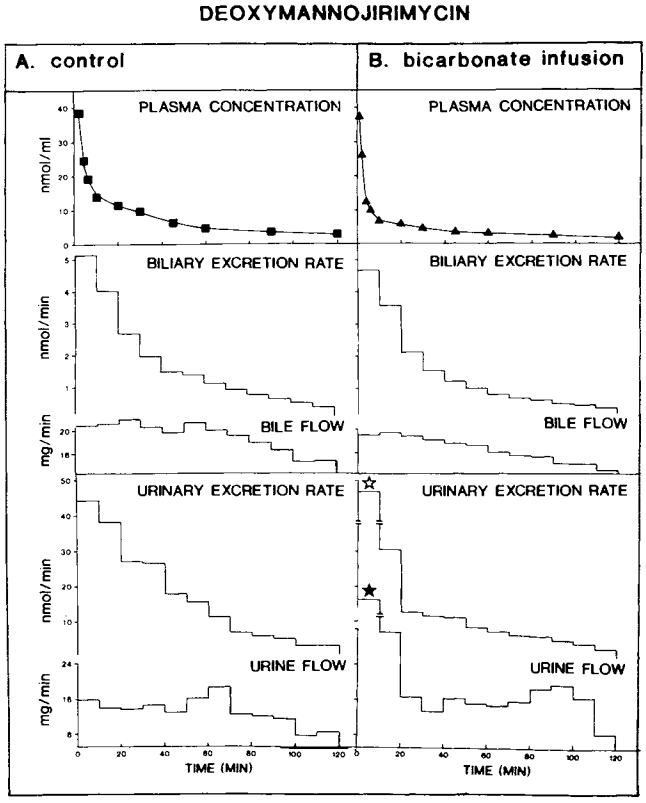

Fig. 2. Basal pharmacokinetic data for dMM in the control situation (A) and after bicarbonate administration (B). Decay in plasma concentration (nmol/ml), biliary and urinary excretion rate (nmol/min), and flow of bile and urine (mg/min) are shown. The scale of the *y* axis applies to both A and B, except for the bars marked with stars: From 0 to 10 min the average urinary excretion rate of dMM was 86.9 nmol/min (open star) and the average urine flow was 58.6 mg/min (filled star).

of the dose was excreted in the urine, with 52 ± 3% of the dose of dMM excreted at the end of the experiment (mean ± SE; $n = 6$). This is shown in Table I as the fraction excreted in urine in 2 hr ($fe_{u,2hr}$).

In all experiments (except where the renal vessels were ligated; see below) bile flow was fairly constant, with final flow rates never below 70% of the starting value (see Figs. 2 and 4). Biliary excretion of dMM (Fig. 2A) was approximately 10% of urinary excretion; an average of 4.9 ± 0.6% of the injected dose was recovered from the bile after 120 min in the control situation, shown in Table I as the fraction excreted in bile in 2 hr ($fe_{b,2hr}$).

Small fractions of the dose were found in the collected organs and plasma after 120 min (Fig. 5), liver and kidneys showing the highest contribution, with 2.1 ± 0.4 and 1.1 ± 0.5% of the dose, respectively (mean ± SE; $n = 3$). To get a better view of the relative accumulation of the compounds, the absolute values in Fig. 5 were converted to tissue/plasma concentration ratios (Fig. 6), by dividing the drug content of each organ (nmol) by the volume of that organ (ml; assuming $m/v = 1$) and, subsequently, by the plasma concentration. Figure 6 shows that the kidneys effectively concentrated dMM, with a tissue/plasma concentration ratio of 5.8, compared to 2 for the other collected tissues.

During the saline infusion, the $fe_{u,2hr}$ was equal to controls, although urine flow was four to five times lower (mean value, 3.0 mg/min). Since a low and irregular urine flow prohibits precise calculation of the renal clearance, this value is not shown in Table I for saline experiments. In total, 53% of the dose was excreted in urine and 6.0% in bile (Table I; mean of two experiments). These values are not significantly different from controls. Furthermore, the plasma concentration–time curve showed the same profile as the control curve, with $t_{1/2_1} = 3.1$ min and $t_{1/2_2} = 49$ min (results not shown). Finally, the tissue distribution of dMM after saline infusion did not differ significantly from the experiments with a mannitol infusion.

We studied the effect of alkalinization of the urine on the excretion of both compounds by the kidneys. In control experiments, urine pH was about 6. Infusion of bicarbonate raised the urine pH to 7.5–8.5. This value did not drop below 6.5 at the end of the experiment. At pH 6, only 6% of dMM is present in the uncharged form, compared to 86% at pH 8. Since this is the form that could, in principle, facilitate passive back-diffusion and/or carrier-mediated reabsorption (e.g., by sugar-type carrier systems) from the primary urine by renal tubular cells, a reduction of dMM excretion via the kidneys at alkaline conditions could be anticipated. However, the distribution and elimination patterns of dMM (Fig. 2B) closely resembled those of the control situation. Plasma half-lives were comparable: 1.5 ± 0.2 min ($t_{1/2_1}$) and 57 ± 6 min ($t_{1/2_2}$) (mean ± SD; $n = 3$). The increased urine flow during the first 30 min also did not significantly change the urinary excretion of dMM, which amounted to 31 ± 2% of the dose after 30 min and 47 ± 5% of the dose after 120 min, respectively ($P > 0.05$ compared to controls). The amount of drug excreted in bile (4.2 ± 0.4% of dose) was similar to controls. dMM accumulated slightly less in the collected tissues (results not shown), but this was significant only for the intestine ($P < 0.05$).

However, when the renal vessels were ligated a different elimination pattern was found. The $t_{1/2_1}$ of dMM, reflecting mainly distribution, did not significantly differ from controls: 4.1 ± 0.9 min (mean ± SD; $n = 3$). As expected, the second phase of the plasma disappearance curve was changed dramatically (Fig. 3A): the $t_{1/2_2}$ was over 260 min. Plasma levels tended to reach a plateau level after 30 min, of approximately 18 μ*M*, resulting in a percentage of dose remaining in plasma that was four to five times higher than controls ($P < 0.01$). The average biliary excretion of dMM was decreased by 35%, to 3.2 ± 0.9% of the dose after 120 min ($P > 0.05$ compared to controls), probably related to the lower bile flow. Ligation of the kidneys inevitably led to a decline in bile flow, however the size varied between the experiments, from 48 to 86 to 91% decrease after 2 hr, compared to the starting value. The percentage of dose remaining in the organs after 120 min was significantly higher than controls for all organs: liver, 3–4 times ($P < 0.05$); intestine, 2–3 times ($P < 0.01$); heart, 3 times ($P < 0.001$); and stomach, 1.4 times ($P < 0.05$) (results not shown).

N-Methyl-1-Deoxynojirimycin

After intravenous administration of [^{14}C]MedNM, radioactivity also was eliminated from the plasma in a biexpo-

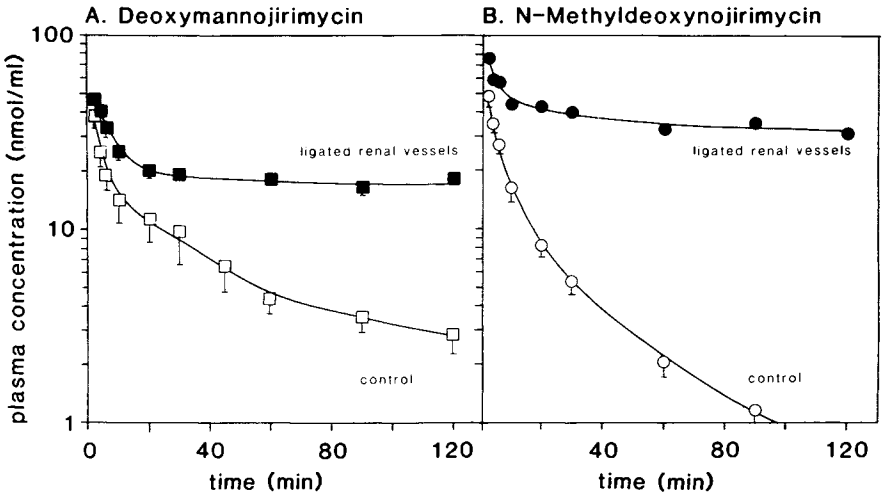

Fig. 3. Plasma disappearance patterns of dMM (A) and MedNM (B). The control situation (open symbols) is compared with the situation where the renal route of excretion is eliminated by a ligature of the renal afferent blood vessels (filled symbols). Data are mean values; SE is only shown when exceeding size of symbols.

nential fashion in all four experimental situations (Figs. 3B and 4A; saline results not shown). For mannitol infusions (control) $t_{1/2_1}$ = 4.5 ± 1.9 min and $t_{1/2_2}$ = 32 ± 8 min (mean ± SD of seven experiments). Figure 4A shows that MedNM also appeared in the urine almost instantaneously and in even higher amounts than did dMM. After 30 min 60 ± 8% of the dose was excreted in the urine, increasing to 80 ± 6% at the end of the experiment. Earlier work with the parent compound dNM (pilot experiments in cats) showed that this compound also disappeared rapidly from the blood and was found unchanged in urine (J. J. Neefjes, unpublished observations). For MedNM biliary excretion was of minor importance: Only 0.16 ± 0.02% of the dose reached the bile after 120 min. Small fractions of the dose were recovered from the various organs, ranging from 0.9 ± 0.1% for the kidneys to 0.02 ± 0.01% for the heart (Fig. 5). MedNM was highly concentrated in kidneys compared to the plasma concentration, displaying a tissue/plasma concentration ratio of 18, compared to 2 for the other organs.

Comparative studies with an infusion of 0.154 *M* saline showed no significant differences from the experiments performed with a 5% mannitol infusion. Half-lives in plasma were 4.9 ($t_{1/2_1}$) and 29 ($t_{1/2_2}$) min, respectively, and total urinary and biliary excretions were comparable: 64 and 0.19%, respectively (mean of two experiments; Table I). Tissue distribution also did not differ from controls.

Table I. Comparison of the Pharmacokinetic Parameters Clearance, Cl (ml/min; Mean ± SD Calculated as Described Under Materials and Methods), Volume of Distribution of the Elimination Phase, V_β, and at Steady State V_{ss} (ml), and Fraction Excreted in Urine, $fe_{u,2hr}$, or Bile, $fe_{b,2hr}$, in 2 hr of the Compounds dMM and MedNM

	dMM			MedNM		
Total body	Cl	V_β	V_{ss}	Cl	V_β	V_{ss}
Control	4.16 ± 0.37	307	265	6.32 ± 0.36	296	164
Saline	4.80 ± 0.21	339	262	6.47 ± 0.83	272	170
Bicarbonate	6.21 ± 0.30	514	437	5.85 ± 0.46	250	169
Nephrectomized	0.23 ± 0.24	206	201	0.26 ± 0.13	94	93
Renal excretion	Cl	$fe_{u,2hr}$		Cl	$fe_{u,2hr}$	
Control	2.63 ± 0.58	0.515		6.83 ± 0.54	0.803	
Bicarbonate	2.78 ± 0.46	0.466		5.33 ± 0.85	0.902	
Saline	ND[a]	0.528		ND	0.635	
Hepatic excretion	Cl	$fe_{b,2hr}$		Cl	$fe_{b,2hr}$	
Control	0.26 ± 0.02	0.049		0.012 ± 0.0005	0.002	
Bicarbonate	0.30 ± 0.05	0.042		0.012 ± 0.0008	0.002	
Saline	0.37 ± 0.02	0.060		0.014 ± 0.0010	0.002	
Nephrectomized	0.03 ± 0.01	0.032		0.004 ± 0.0005	0.005	

[a] Not determinable.

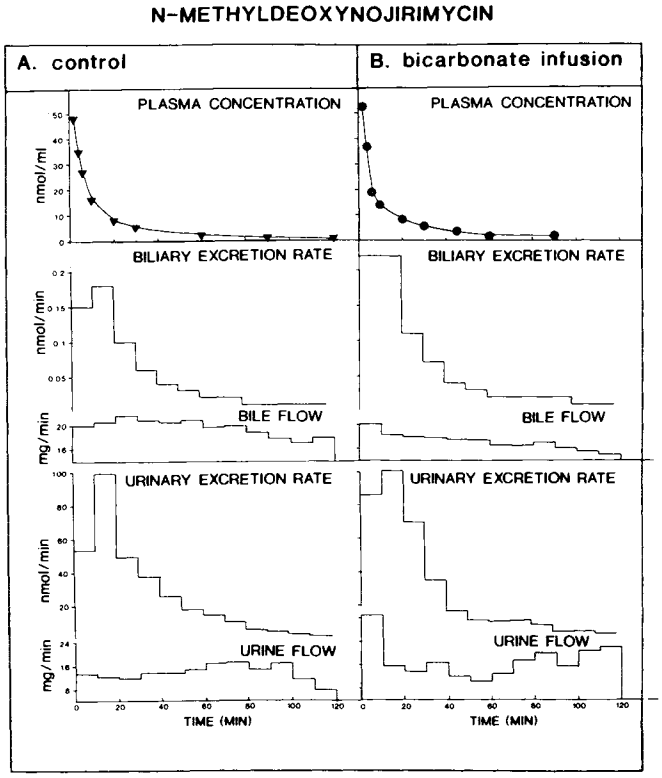

Fig. 4. Basal pharmacokinetic data for *N*-methyl-1-deoxynojirimycin in the control situation (A) and after bicarbonate administration (B). Details are as in the legend to Fig. 2. The scale of the *y* axis applies to both A and B.

Elevation of the urine pH, as described above, increased the percentage of MedNM molecules in the uncharged form from 29 to 98%, respectively. However, the pharmacokinetic parameters calculated (Table I) did not differ from controls. Half-lives in plasma were $t_{1/2_1}$ = 2.8 ± 1.2 min and $t_{1/2_2}$ = 30 ± 6 min (mean ± SD; n = 3). Urinary excretion showed the same pattern as controls: 64 ± 7% of

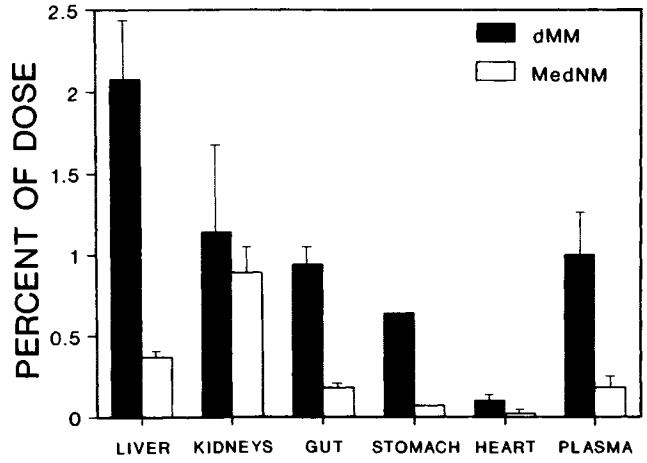

Fig. 5. The percentage of the dose of dMM (black bars) and MedNM (white bars) present in the collected tissues and plasma at 120 min after i.v. administration. Mean values of three (dMM) or seven (MedNM) experiments; the SE is shown only when it exceeds the size of symbols.

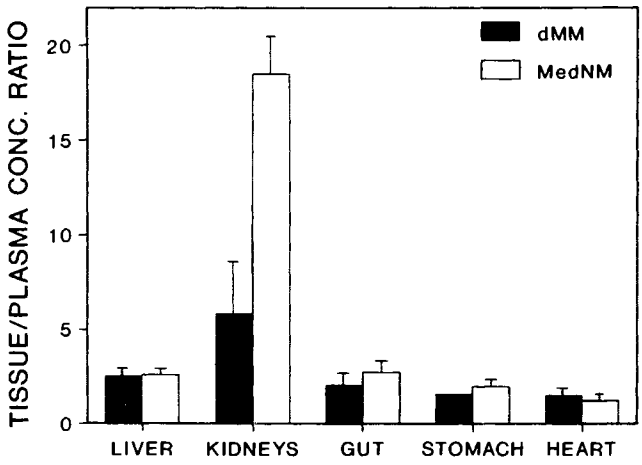

Fig. 6. The accumulation of dMM (black bars) and MedNM (white bars) in tissue, expressed as the ratio of the concentration in each organ and the plasma concentration at 120 min after i.v. administration. Mean values of three (dMM) or seven (MedNM) separate experiments; the SE is shown only when it exceeds the size of symbols.

the dose was excreted in the urine after 30 min, while after 120 min 90 ± 4% was excreted. Biliary excretion was also unchanged: After 120 min 0.20 ± 0.03% of the dose had been eliminated. Finally, the distribution of MedNM over the various tissues also did not deviate from control values (results not shown).

When the renal vessels were ligated the plasma disappearance pattern changed drastically (see Fig. 3B), especially in the second phase of the curve. A plateau value was reached for the plasma concentration after 30 min of approximately 35 μM, resulting in a 40-fold increase in the percentage of MedNM still present in the plasma after 120 min compared to controls. The $t_{1/2_1}$ was not changed significantly from control (2.9 compared to 4.5 min). However, the $t_{1/2_2}$ exceeded 100 min in the two separate experiments. The average percentage of the dose recovered in bile, 0.53%, was significantly higher than controls ($P < 0.01$), although in one of the experiments bile flow decreased by 75% (resulting $fe_{b,2hr}$ = 0.004). Except for the kidneys, accumulation of MedNM in all collected organs was significantly higher than control values ($P < 0.001$). The percentage of the dose remaining in the liver, intestine, stomach, and heart was increased 10- to 13-fold compared to control values (results not shown).

Calculation of the Glomerular Filtration Rate

The plasma concentration of [^{14}C]mannitol was measured at the same time points used for the other experiments. Steady-state values were reached within the stabilization period and remained constant for at least 2 hr. From the steady-state plasma concentration and the rate of infusion, the plasma clearance of mannitol was calculated [Eq. (4)] for all time points and averaged for each experiment. The glomerular filtration rate was found to be 2.60 ± 0.41 ml/min (mean ± SD; n = 4).

Metabolism Studies

Both compounds were recovered unchanged from the

urine. MedNM (R_f value, 0.28) was stable for prolonged periods of time after incubation with blank urine at 20°C and when urine samples were stored at −20°C (for up to 2 years) and no metabolites of MedNM were found in bile. dMM (R_f value, 0.23) was stable in urine and bile when stored at 20°C for 24 hr: however, after 3 weeks R_f values had shifted to 0.15 (bile) and 0.10 (urine). The same R_f shift was seen in urine samples from *in vivo* experiments when stored for 6 weeks at −20°C. There is preliminary evidence that dMM is (partially) metabolized in rat liver, but the total fraction metabolized represents less than 5% of total dose. As mentioned earlier, no metabolites were detected in urine.

DISCUSSION

Pharmacokinetic Analysis

The pharmacokinetic parameters V_β, V_{SS}, $fe_{u,2hr}$, and $fe_{b,2hr}$ (Table I) and $t_{1/2_1}$ and $t_{1/2_2}$ of the control experiments, compared with results from saline infusions, indicate that mannitol did not interfere with the distribution and elimination of the compounds under study.

Both dMM and MedNM showed rapid plasma disappearance that could be fitted best by a two-compartment kinetic model (simultaneous fitting of all data, and individual curves). However, for dMM the mean plasma curve could be fitted significantly better (as compared with an F test) with a three-compartment model. An indication for this third, "deep" compartment can also be found in the fact that the $fe_{u,2hr}$ for dMM was only 0.515, compared to 0.803 for MedNM. Therefore it is possible that there is a deep storage compartment for dMM and that intracellular accumulation in certain tissues, including the kidneys, accounts for the third, slow phase in the mean plasma curve. Such a slow elimination process was confirmed in additional experiments over a prolonged period of time (8 hr), showing that another 19% of the dose of dMM is excreted in the urine and an extra 1.4% in bile in the following 6 hr. For these reasons it is likely that eventually all of the dMM will be recovered in urine and bile at a ratio close to 10:1.

Routes of Elimination

Elimination of both compounds occurred preferentially from the central compartment by the kidneys, as demonstrated in Fig. 3, whereas plasma concentrations quickly reached a plateau when the renal vessels were ligated. The central volume of distribution (V_1) of both compounds (data not shown) was almost equal to the sum of blood volume [64 ml/kg rat (22)] and extracellular fluid [18–22% of body weight (24)]. Both dMM and dNM equilibrate rapidly across cellular plasma membranes through nonfacilitated diffusion (11,15). Since some dNM derivatives, like MedNM, are more potent than dNM itself (25), their rate of cellular uptake is unlikely to be less than that of dNM. Hence the V_{SS} (values shown in Table I) approximately equals the total-body volume of the rat for most experimental situations. However, this does not imply that dMM and MedNM distribute evenly over all body tissues. Both compounds exhibited a higher concentration ratio in the kidneys than in the other tissues collected (see Fig. 6). The importance of the kidneys for the elimination of dMM and MedNM was also supported by the finding that, after ligation of the renal vessels, V_{SS} decreased (and also V_β, but this parameter is not elimination independent) by 60–70 ml compared to controls ($P < 0.05$ when individual curves were fitted and compared). For MedNM, this reduction of V_{SS} by 70 ml can be explained by the contribution of the kidneys to the steady-state volume of distribution, since the volume of the kidneys (1% of total body weight) multiplied by the concentration ratio of MedNM in the kidneys (18.5; Fig. 6) yields a "kidney distribution volume" of approximately 50 ml. For dMM this calculation resulted in a lower value (16 ml), but here experimental variability was considerable. The hepatic route of elimination was of less significance for both compounds: For dMM hepatic clearance was 10% of renal clearance, and for MedNM its contribution to the total-body clearance was negligible.

Mechanisms of Renal Excretion

Differences in urine flow (Figs. 2 and 4) did not significantly change the $fe_{u,2hr}$ for dMM and MedNM (Table I). The $fe_{u,2hr}$ was also not changed when higher doses, 10 and 20 μmol, were given (data not shown). In addition, no linear relationship was found when urine flow was plotted against clearance for each experimental situation.

The basic sugar analogue MedNM possesses a tertiary amine function with a pK_a of 6.3–6.4 (17) and dMM contains a secondary amine function with a pK_a of 7.2 (16). Consequently, at pH 7.4 the compounds are present partially in the protonated (cationic) form (Fig. 1). The present results indicate that the ionization status of dMM and MedNM in the primary urine is unimportant to their renal handling (Figs. 2 and 4), implying the absence of tubular reabsorption via passive diffusion. In the absence of active transport both compounds are probably too polar, even in their neutral form, to be rapidly reabsorbed (24).

Renal clearance of dMM was found to be similar to the glomerular filtration rate. This was not the case for MedNM, where the renal clearance was at least twice the glomerular filtration rate, indicating that active tubular secretion may be involved. Such secretory processes are located predominantly along the proximal tubule, and both acid and base transport systems appear to be multispecific (24,26). Assuming that the cation tubular secretion system is involved, it seems surprising that MedNM (9% in the cationic form) is more efficiently secreted than dMM (39% in the cationic form at pH 7.4; see Fig. 1). However, not only the concentration of the cationic form but also the relative affinity for the proposed carrier plays a decisive role. The presence of a methyl group on the nitrogen center may be crucial in this respect (27).

Total-body clearance of MedNM was equal to the sum of renal and hepatic clearance, which implies that there is no other, quantitatively important, route of elimination for MedNM. Initially dMM seemed to deviate from this pattern: Renal and biliary clearance together made up only 75% of the total-body clearance (Table I). As discussed above, there are indications for a third, slow phase of the plasma disappearance curve of dMM. In that case, the actual area under the curve will be underestimated, and consequently the actual total-body clearance is smaller than the value shown in Table I. Theoretically there could be an additional route of

elimination to make up for the difference in clearance. However, if such a route exists, it is of little significance. As shown in Fig. 3A, no further plasma decay occurs when the renal route of elimination is cut off. Elimination via the intestine is not likely to occur in significant amounts taking into account the low amounts recovered from the small intestine (Figs. 5 and 6). Furthermore, it is not likely that biotransformation is responsible for the discrepancy, since the radioactive label of dMM is introduced in such a way that it cannot easily be displaced or removed. Radioactive metabolites would be expected to be in plasma, urine, and bile and to contribute to the total clearance.

Mechanisms of Hepatic Excretion

Biliary excretion of both compounds was related to bile flow. This is best illustrated in experiments where the renal vessels were ligated, where one would expect an increased biliary excretion when elimination via the urine is blocked. In this situation for dMM the concentration in plasma (central compartment) increased four to five times. Consequently, the concentration in the liver (peripheral compartment) was also increased (three to four times; $P < 0.05$), resulting in an enhanced driving force for elimination from this compartment. Indeed the concentration of dMM in bile was three to six times higher than control values, but $fe_{b,2hr}$ was less elevated probably due to the decline in bile flow caused by ligation of the renal vessels. This rigorous procedure, in combination with regular blood sampling, may cause a steady decline in blood pressure and in bile flow. For MedNM the mean plasma concentration was increased 40 times, whereas the liver concentration was increased only 12 times ($P < 0.001$) and the mean bile concentration was 17 times higher after ligation of the renal vessels. Here the $fe_{b,2hr}$ was significantly increased ($P < 0.01$) but not linear with the plasma concentration. To investigate if this discrepancy was the result of rate-limiting canalicular excretion, control studies were performed with higher doses of dMM. After dosages of 10 and 20 μmol of dMM, the corresponding $fe_{b,2hr}$ values were similar to those of 4-μmol controls, namely, 0.048 for both doses (mean values of two experiments). Thus under control conditions the transport from liver to bile does not seem to be saturated. Experiments with dMM and MedNM in isolated perfused rat livers support these data, since linear kinetics were found for doses ranging from 4 to 40 μmol (E. Faber, manuscript in preparation). A third possibility is that the biliary excretion and/or hepatic uptake of the model compounds is inhibited by endogenous compounds that accumulate in the circulation after ligation of the renal vessels. Therefore it is likely that the ligation procedure itself can be held responsible for the discrepancy.

Tissue Accumulation and Retention

With regard to the tissue distribution, dMM and MedNM behave quite differently. The secondary amine dMM is present in larger amounts 120 min after injection in all tissues collected, compared to MedNM (Fig. 5). The liver content could be corrected for the amount of drug present in the biliary tree [a known volume of 0.32% of liver weight (28)], but this contribution was very small for both dMM (1.1%) and MedNM (0.15%). For the kidneys similar calculations led us to the conclusion that the contribution of drug present in the urinary lumen, 120 min after injection, to the total kidney content was small.

Relating the amount of drug in an organ to the volume of that organ enabled us to calculate the tissue/plasma concentration ratio, as shown in Fig. 6. Neither dMM nor MedNM displayed a homogeneous distribution over the various organs: For both, considerable concentrations occurred in the kidneys. This is not surprising, since both compounds are eliminated via the kidneys and some retention of compound can be expected. In addition, MedNM is probably actively secreted by the renal tubular cells, and for many organic cations, this process involves an active concentrative secretion across the brush border membrane (lumenal side) (26). There may also be specific transporters on the basolateral membrane to move organic cations from blood to the renal cell. In addition, liver and kidney comprise a large pool of acidic endocytic vesicles (endosomes, lysosomes) that are capable of trapping tertiary and secondary amines by protonation. Preliminary data obtained through subcellular fractionation showed that dMM is concentrated to some extent in the lysosomal fraction of the rat liver, whereas MedNM concentrated even more in lysosomes and microsomes (E. Faber, unpublished observations). Whether such compartments are relevant for therapeutic effect remains to be established.

On the basis of a two-compartment kinetic model for MedNM and dMM, it can be calculated that a constant infusion of 4.0 and 2.5 mg/hr of MedNM and dMM, respectively, would lead to steady-state plasma concentrations in the range of 20–100 μ*M*, where dNM and *N*-hydroxyethyl-dNM are reported to inhibit hepatic glycogenolyses in the rat (14). The two compounds mentioned above also inhibit sucrase activity in rats, and a constant infusion of 20 and 12 μg/hr of MedNM and dMM is required to reach steady-state plasma concentrations in the reported therapeutic range of 0.2–0.4 μ*M* (6).

In conclusion, for both dMM and MedNM, renal elimination is the major route of elimination, and for MedNM tubular secretion appears to play a significant role. The volume of distribution of both compounds is close to the total-body volume, however, significant accumulation occurs in the kidneys. In spite of efficient renal clearance, dMM may be quite slowly eliminated from the body because of persistent storage in "deep" intracellular compartments.

ACKNOWLEDGMENT

Dr. Hans Proost is gratefully acknowledged for the valuable discussions and for putting the computer program MULTIFIT at our disposal.

NOMENCLATURE

$t_{1/2_1}$	Initial half-life
$t_{1/2_2}$	Terminal half-life
$fe_{u,2hr}$	Fraction excreted in urine in 2 hr
$fe_{b,2hr}$	Fraction excreted in bile in 2 hr
V_β	Volume of distribution of the elimination phase
v_{ss}	Volume of distribution at steady state

REFERENCES

1. U. Fuhrmann, E. Bause, and H. L. Ploegh. Inhibitors of oligosaccharide processing. *Biochim. Biophys. Acta* 825:95–110 (1985).
2. A. D. Elbein. Inhibitors of the biosynthesis and processing of N-linked oligosaccharide chains. *Annu. Rev. Biochem.* 56:497–534 (1987).
3. V. Gross, T. Andus, T. A. Tran-Thi, R. T. Schwarz, K. Decker, and P. C. Heinrich. 1-Deoxynojirimycin impairs oligosaccharide processing of α1-proteinase inhibitor and inhibits its secretion in primary cultures of rat hepatocytes. *J. Biol. Chem.* 258:12203–12209 (1983).
4. V. Gross, T. A. Tran-Thi, R. T. Schwarz, A. D. Elbein, K. Decker, and P. C. Heinrich. Different effects of the glucosidase inhibitors 1-deoxynojirimycin, N-methyl-1-deoxynojirimycin and castanospermine on the glycosylation of rat α1-proteinase inhibitor and α1-acid glycoprotein. *Biochem. J.* 236:853–860 (1986).
5. J. B. Parent, T. K. Yeo, K. T. Yeo, and K. Olden. Differential effects of 1-deoxynojirimycin on the intracellular transport of secretory glycoproteins of human hepatoma cells in culture. *Mol. Cell. Biochem.* 72:21–33 (1986).
6. K. M. Robinson, B. L. Rhinehart, M. E. Begovic, C. H. R. King, and P. S. Liu. Castanospermine-glucosides are potent, selective, long-acting sucrase inhibitors. *J. Pharmacol. Exp. Ther.* 251:224–229 (1989).
7. G. Heinz, M. Komjati, A. Korn, and W. Waldhausl. Reduction of postprandial blood glucose by the α-glucosidase inhibitor Miglitol (BAY m 1099) in Type II diabetes. *Eur. J. Clin. Pharmacol.* 37:33–36 (1989).
8. M. J. Humphries, K. Matsumoto, S. L. White, and K. Olden. Inhibition of experimental metastasis by castanospermine in mice: Blockage of two distinct stages of tumor colonization by oligosaccharide processing inhibitors. *Cancer Res.* 46:5215–5222 (1986).
9. R. A. Gruters, J. J. Neefjes, M. Tersmette, R. E. Y. De Goede, A. Tulp, H. G. Huisman, F. Miedema, and H. L. Ploegh. Interference with HIV-induced syncytium formation and viral infectivity by inhibitors of trimming glucosidase. *Nature* 330:74–77 (1987).
10. L. Ratner, N. Van der Heyden, and D. Dedera. Inhibition of HIV and SIV Infectivity by blockade of alpha-glucosidase activity. *Virology* 181:180–192 (1991).
11. J. J. Neefjes, J. Lindhout, H. J. G. Broxterman, G. A. Van der Marel, J. H. Van Boom, and H. L. Ploegh. Non-carrier-mediated uptake of the mannosidase I inhibitor 1-deoxymannojirimycin by K562 erythroleukemic cells. *J. Biol. Chem.* 264:10271–10275 (1989).
12. R. Saul, R. J. Molyneux, and A. D. Elbein. Studies on the mechanism of castanospermine inhibition of α- and β-glycosidases. *Arch. Biochem. Biophys.* 230:668–675 (1984).
13. U. Fuhrmann, E. Bause, G. Legler, and H. L. Ploegh. Novel mannosidase inhibitor blocking conversion of high mannose to complex oligosaccharides. *Nature* 307:755–758 (1984).
14. M. Bollen, A. Van de Broeck, and W. Stalmans. 1-Deoxynojirimycin and related compounds inhibit glucogenolysis in the liver without affecting the concentration of phosphorylase a. *Biochem. Pharmacol.* 37:905–909 (1988).
15. M. Bollen and W. Stalmans. The antiglycogenolytic action of 1-deoxynojirimycin results from a specific inhibition of the α-1,6-glucosidase activity of the debranching enzyme. *Eur. J. Biochem.* 181:775–780 (1989).
16. G. Legler and E. Juelich. Synthesis of 5-amino-5-deoxy-D-mannopyranose and 1,5-di-deoxy-1,5-imino-D-mannitol, and inhibition of alpha- and beta-D-mannosidases. *Carbohydr. Res.* 128:61–72 (1984).
17. J. Schweden, C. Borgmann, G. Legler, and E. Bause. Characterization of calf liver glucosidase I and its inhibition by basic sugar analogues. *Arch. Biochem. Biophys.* 248:335–340 (1986).
18. R. M. Ruprecht, L. D. Bernard, R. Bronson, M. A. G. Sosa, and S. Mullaney. Castanospermine vs its 6-O-Butanoyl analog—A comparison of toxicity and antiviral activity *in vitro* and *in vivo*. *J. Acquir. Immune Defic. Syndr.* 4:48–55 (1991).
19. H. J. G. Broxterman, J. J. Neefjes, G. A. Van der Marel, H. L. Ploegh, and J. H. Van Boom. Synthesis of the antibiotic 1,5-dideoxy-1,5-imino-D-mannitol. *J. Carbohydr. Chem.* 7:593–603 (1988).
20. C. Neef, R. Oosting, and D. K. F. Meijer. Structure-pharmacokinetics relationship of quaternary ammonium compounds. Elimination and distribution characteristics. *Naunyn Schmiedebergs Arch. Pharmacol.* 328:103–110 (1984).
21. G. J. Mulder, E. Scholtens, and D. K. F. Meijer. Collection of metabolites in bile and urine from the rat. In W. B. Jakoby (ed.), *Methods in Enzymology, Vol. 77,* Academic Press, New York, 1981, pp. 21–30.
22. W. S. Bivin, M. P. Crawford, and N. R. Brewer. Morphophysiology. In H. J. Baker, J. R. Lindsey, and S. H. Weisbroth (eds.), *The Laboratory Rat,* Academic Press, New York, 1979, pp. 73–103.
23. C. Neef and D. K. F. Meijer. Structure-pharmacokinetics relationship of quaternary ammonium compounds. Correlation of physicochemical and pharmacokinetic parameters. *Naunyn Schmiedebergs Arch. Pharmacol.* 328:111–118 (1984).
24. M. Rowland and T. N. Tozer. *Clinical Pharmacokinetics: Concepts and Applications,* Lea & Febiger, Philadelphia/London, 1989.
25. A. Tan, L. van den Broek, C. Van Boeckel, H. Ploegh, and J. Bolscher. Chemical modification of the glucosidase inhibitor 1-deoxynojirimycin: structure-activity relationships. *J. Biol. Chem.* 266:14504–14510 (1991).
26. C. A. M. Van Ginneken and F. G. M. Russel. Saturable pharmacokinetics in the renal excretion of drugs. *Clin. Pharmacokinet.* 16:38–54 (1989).
27. L. Peters. Renal tubular excretion of organic bases. *Pharmacol. Rev.* 12:1–35 (1960).
28. E. L. Forker. Hepatocellular uptake of inulin, sucrose and mannitol in rats. *Am. J. Physiol.* 219:1568–1573 (1970).